A Convex Relaxation Approach to Optimal Placement of Phasor Measurement Units

Vassilis Kekatos and Georgios B. Giannakis
Dept. of ECE, University of Minnesota
Minneapolis, MN 55455, USA
Emails:{kekatos,georgios}@umn.edu

***Abstract*—Instrumenting power networks with phasor measurement units (PMUs) facilitates several tasks including optimum power flow, system control, contingency analysis, visualization, and integration of renewable resources, thus enabling situational awareness – one of the key steps toward realizing the smart grid vision. The installation cost of PMUs currently prohibits their deployment on every bus, which in turn motivates their strategic placement across the power grid. As state estimation is at the core of grid monitoring, PMU deployment is optimized here based on estimation-theoretic criteria. Considering both voltage and current PMU readings and incorporating conventionally derived state estimates under the Bayesian framework, PMU placement is formulated as an optimal experimental design task. To obviate the combinatorial search involved, a convex relaxation is also developed to obtain solutions with numerical optimality guarantees. In the tests performed on standard IEEE 14- and 118-bus benchmarks, the proposed relaxation is very close to and oftentimes attains the optimum.**

I. Introduction

Phasor measurement units are contemporary metering devices installed on system buses to measure phasors of bus voltages and currents flowing across lines [13], [6]. Merits of PMUs (a.k.a. synchrophasors) over conventional power meters include increased precision in measuring phasor angles due to network-wide synchronization and higher sampling rates.

PMU penetration has so far been rather limited, mainly because of the installation and networking costs involved. However, their important role in network operation and the growing maturity of PMU technology are expected to markedly increase their deployment [4]. According to the North American Synchrophasor Initiative, the number of PMUs installed and networked in the eastern/western interconnection will likely raise from 105/56 as of 2009 to 400-600 by 2014 [11].

Strategic placement of synchrophasors is currently a critical issue for the power operators worldwide, and has been considered in the context of topological observability (existence of a spanning measurement tree) [2], and incomplete observability [12]. Building on these notions, optimal PMU placement has been posed as a binary linear program [7]; as a binary quadratic one [5]; or as a stochastic optimization problem [1].

In this work, PMU sites are selected purely based on estimation-theoretic criteria. Estimating the power grid state is traditionally performed by the supervisory control and data acquisition (SCADA) center based on conventional meter readings [16, Ch. 12]. The improvement in estimation accuracy by combining PMU and SCADA measurements has been documented in [17]. Similar to [10], PMU placement is formulated here as a variation of the optimal experimental design problem [14], [3, Sec. 7.5]. After posing system state estimation as a linear regression problem, SCADA-based estimates are utilized as Gaussian priors (Section II). PMU placement is then optimized by minimizing the error covariance matrix (Section III). The combinatorial problem involved is suboptimally solved after relaxing it to a convex semidefinite program (SDP) [3], [8]. The SDP-derived cost value yields bounds on the suboptimality gap. Surprisingly, the numerical results of Section V show that this gap is small or oftentimes zero for the IEEE 14- and 118-bus power network benchmarks [15]. In contrast, the approach of [10] ignores current measurements of PMU lines, and estimates only the phase of the system state using a greedy algorithm.

Notation: Lower- (upper-) case boldface letters denote column vectors (matrices), and calligraphic letters stand for sets; $\mathbf{1}_N$ ($\mathbf{0}_N$) denotes the all-ones(zeros) vector of length N; $(\cdot)^T$ and $(\cdot)^\star$ transposition and complex conjugation, respectively; $\mathcal{N}(\mathbf{m},\mathbf{\Sigma})$ stands for the multivariate Gaussian probability density function with mean $\mathbf{m}$ and covariance matrix $\mathbf{\Sigma}$.

II. PMU-based State Estimation

Consider a power grid consisting of N_b buses connected through N_l transmission lines. The problem of estimating the state of the grid is equivalent to estimating the complex voltages across its buses. In rectangular coordinates, the system state is described by the $2N_b \times 1$ vector $\mathbf{v}_o := [\mathbf{v}_{o,r}^T \ \mathbf{v}_{o,i}^T]^T$, where $\mathbf{v}_{o,r}$ and $\mathbf{v}_{o,i}$ comprise the real and imaginary parts of nodal voltages, respectively.

Consider the PMU measurements collected at the n-th bus. Without loss of generality, these readings include the complex bus voltage and the complex currents flowing over the L_n lines incident to the n-th bus. The synchrophasor measurements in rectangular coordinates are collected in the vector $\mathbf{z}_n \in \mathbb{R}^{M_n}$ with $M_n := 2(L_n+1)$, and obey the following linear model

$$\mathbf{z}_n = \mathbf{H}_n \mathbf{v}_o + \mathbf{w}_n \tag{1}$$

where $\mathbf{H}_n \in \mathbb{R}^{M_n \times 2N}$ is the associated regression matrix, and $\mathbf{w}_n \sim \mathcal{N}(\mathbf{0}, \mathbf{\Sigma}_n)$ denotes the additive Gaussian noise vector

Dr. Kekatos' work was supported by the Marie Curie International Outgoing Fellowship No. 234914 within the 7-th European Community Framework Programme. This work was also supported by NSF grants CCF-0830480, 1016605, and ECCS-0824007, 1002180.

that is assumed independent across PMUs.

To capture presence or absence of a PMU, a binary variable a_n is introduced per bus: its value is 1 if a PMU is present at the n-th bus; and 0, otherwise. For a given PMU indicator vector $\mathbf{a} := [a_1 \ \cdots \ a_{N_b}]^T$, the maximum likelihood estimate (MLE) of the system state obeying the linear-Gaussian model (1), is

$$\hat{\mathbf{v}}_{\text{MLE}} = \mathbf{A}^{-1} \left(\sum_{n=1}^{N_b} a_n \mathbf{H}_n^T \mathbf{\Sigma}_n^{-1} \mathbf{z}_n \right) \tag{2}$$

where matrix $\mathbf{A}$ (assumed non-singular) is given by

$$\mathbf{A} := \sum_{n=1}^{N_b} a_n \mathbf{H}_n^T \mathbf{\Sigma}_n^{-1} \mathbf{H}_n. \tag{3}$$

Invertibility of $\mathbf{A}$ apparently depends on the non-zero entries of $\mathbf{a}$. As the number of PMUs is small, especially during their initial deployment phase, system identifiability is at risk. By incorporating SCADA measurements however, it is possible to regularize the system matrix, and thus enable state estimation even when $\mathbf{A}$ is singular [17]. Nonetheless, simply aggregating SCADA and PMU readings faces three challenges: (i) SCADA measurements are available every 1–5secs, whereas PMU ones are sampled every 0.1–0.2secs [4]; (ii) explicitly including conventional measurements results in a nonlinear estimation problem of even higher dimensionality; and (iii) upgrading the existing estimation software to accommodate high-rate PMU readings compromises backward compatibility [17].

These challenges are addressed here using a Bayesian estimation approach. The SCADA-based state estimate $\hat{\mathbf{v}}_s$ expressed in rectangular coordinates is used as prior information for the PMU-based estimation task. Specifically, it is assumed that the actual state vector is distributed as $\mathbf{v}_o \sim \mathcal{N}(\hat{\mathbf{v}}_s, \mathbf{\Sigma}_s)$. Based on the linear model of (1) and the SCADA-based Gaussian prior information, the system state can now be obtained via the maximum a-posteriori probability (MAP) estimate uniquely given by

$$\hat{\mathbf{v}}_p = \mathbf{\Sigma}_p \left(\sum_{n=1}^{N_b} a_n \mathbf{H}_n^T \mathbf{\Sigma}_n^{-1} \mathbf{z}_n + \mathbf{\Sigma}_s^{-1} \hat{\mathbf{v}}_s \right) \tag{4}$$

where the so-called *gain matrix* is defined as [16], [13]

$$\mathbf{\Sigma}_p := \left(\mathbf{A} + \mathbf{\Sigma}_s^{-1} \right)^{-1}. \tag{5}$$

Standard results assure that $\hat{\mathbf{v}}_p \sim \mathcal{N}(\mathbf{v}_o, \mathbf{\Sigma}_p)$ [9].

Phase Alignment: To align the phase of the SCADA-based prior with that of PMU readings, a PMU needs to be installed at the so-called *reference bus* – typically enumerated as first; see also [13]. Once the reference bus has been PMU-instrumented, its measured voltage phase is subtracted from all other PMU readings so that $\text{Im}(v_o^1)$ is artificially set to zero in the PMU-based system state. This clearly implies that $a_1 = 1$ and that $\text{Im}(v_o^1)$ is removed from the state vector. For notational brevity, $\mathbf{v}_o$ will henceforth refer to the reduced $(2N_b - 1) \times 1$ vector, while $\mathbf{H}_n$'s $(\mathbf{A})$ will denote the corresponding matrices obtained after ignoring the $(N+1)$-st column (and row) from the respective matrices of (1) and (3).

III. Optimal PMU Placement

Building on the state estimate in (4), the problem of PMU placement can be now stated as follows. Given

i) a power network of N_b buses (nodes);
ii) matrices $\{\mathbf{H}_n, \mathbf{\Sigma}_n\}_{n=1}^{N_b}$ (cf. (1) and Section IV-A);
iii) the covariance matrix $\mathbf{\Sigma}_s$ (cf. Section IV-B);
iv) an integer k with $k \leq N$,

and assuming a PMU installed at the reference bus, the goal is to choose $(k-1)$ buses to be PMU-instrumented so that the estimation error of (4) is minimized.

PMU placement is cast here as a variation of the optimal experimental design problem [14]. The state estimation error for a specific PMU placement $\mathbf{a}$ has covariance matrix $\mathbf{\Sigma}_p(\mathbf{a}) = \left(\mathbf{A}(\mathbf{a}) + \mathbf{\Sigma}_s^{-1} \right)^{-1}$, where the dependence on $\mathbf{a}$ will be explicitly denoted throughout this section.

Apparently, between two candidate placements $\mathbf{a}$ and $\mathbf{a}'$ with $\mathbf{1}_{N_b}^T \mathbf{a} = \mathbf{1}_{N_b}^T \mathbf{a}' = k$, placement $\mathbf{a}$ is preferable over $\mathbf{a}'$ if $\mathbf{\Sigma}_p(\mathbf{a}') \succeq \mathbf{\Sigma}_p(\mathbf{a})$. But, if $\mathbf{\Sigma}_p(\mathbf{a}') - \mathbf{\Sigma}_p(\mathbf{a})$ is an indefinite matrix, none of the placements is better than the other. To overcome this partial ordering limitation, placements are typically ranked based on a scalar-valued function of $\mathbf{\Sigma}_p(\mathbf{a})$, that is to be minimized [14], [3]. Typical function choices are:

(c1) E-optimal design: $f_E(\mathbf{a}) := \lambda_{\max}(\mathbf{\Sigma}_p(\mathbf{a}))$, where $\lambda_{\max}$ denotes the maximum eigenvalue of $\mathbf{\Sigma}_p(\mathbf{a})$;

(c2) A-optimal design: $f_A(\mathbf{a}) := \text{trace}(\mathbf{\Sigma}_p(\mathbf{a}))$ that is equal to the sum of the eigenvalues of $\mathbf{\Sigma}_p(\mathbf{a})$;

(c3) M-optimal design: $f_M(\mathbf{a}) := \max_i \{[\mathbf{\Sigma}_p(\mathbf{a})]_{ii}\}$ corresponding to the maximum diagonal entry of $\mathbf{\Sigma}_p(\mathbf{a})$; and

(c4) D-optimal design: $f_D(\mathbf{a}) := \log\det(\mathbf{\Sigma}_p(\mathbf{a}))$, where $\det(\cdot)$ denotes matrix determinant.

Details and interesting geometric interpretations regarding choices (c1)-(c4) can be found in [3, Sec. 7.5], [14].

After this scalarization step, the C-optimal PMU placement can be found as the solution of the optimization problem

$$\tilde{\mathbf{a}}_C := \arg\min_{\mathbf{a}} \quad f_C(\mathbf{a}) \tag{6a}$$

$$\text{s.t.} \quad \mathbf{a}^T \mathbf{1}_{N_b} = k, \ a_1 = 1 \tag{6b}$$

$$\mathbf{a} \in \{0,1\}^{N_b} \tag{6c}$$

where $C \in \{E, A, M, D\}$. Unfortunately, solving (6) entails combinatorial complexity [3], [8]. Suboptimal solutions can be obtained by converting the troublesome binary constraint to the box constraint $\mathbf{0}_{N_b} \leq \mathbf{a} \leq \mathbf{1}_{N_b}$ with the inequalities understood entry-wise [3]. Since $\{0,1\}^{N_b} \subset [0,1]^{N_b}$, such a conversion is a *relaxation* of the original problem. After defining the relaxed feasible set $\mathcal{A} := \{\mathbf{a} : \ \mathbf{a}^T \mathbf{1}_{N_b} = k, \ a_1 = 1, \ \mathbf{0}_{N_b} \leq \mathbf{a} \leq \mathbf{1}_{N_b}\}$, the relaxed problem is expressed as

$$\check{\mathbf{a}}_C := \arg\min_{\mathbf{a} \in \mathcal{A}} \quad f_C(\mathbf{\Sigma}_p(\mathbf{a})). \tag{7}$$

The problem in (7) can be efficiently solved as a convex problem for all $C \in \{E, A, M, D\}$ [3], [8]. The convex formulations are presented briefly for completeness.

For the E-optimal design, instead of minimizing $\lambda_{\max}(\mathbf{\Sigma}_p(\mathbf{a}))$, one can alternatively maximize $\lambda_{\min}(\mathbf{\Sigma}_p^{-1}(\mathbf{a}))$

by introducing the auxiliary variable t and solving the SDP

$$(\check{\mathbf{a}}_E, \check{t}_E) := \arg\min_{\mathbf{a}\in\mathcal{A},t} \left\{-t:\ \mathbf{A}(\mathbf{a}) + \mathbf{\Sigma}_s^{-1} \succeq t\mathbf{I}_{2N_b-1}\right\}. \quad (8)$$

For the A-optimal design, minimizing the trace of $\mathbf{\Sigma}_p(\mathbf{a})$ can be accomplished after introducing the auxiliary vector variable $\mathbf{t} := [t_1\ \ldots\ t_{2N_b-1}]$, leading to the SDP

$$(\check{\mathbf{a}}_A, \check{\mathbf{t}}_A) := \arg\min_{\mathbf{a}\in\mathcal{A},\mathbf{t}} \quad \mathbf{t}^T\mathbf{1}_{2N_b-1} \quad (9)$$
$$\text{s.t.} \begin{bmatrix} \mathbf{A}(\mathbf{a})+\mathbf{\Sigma}_s^{-1} & \mathbf{e}_k \\ \mathbf{e}_k^T & t_k \end{bmatrix} \succeq \mathbf{0},\ k = 1,\ldots,2N_b-1.$$

The M-optimal design can be suboptimally solved by the SDP

$$(\check{\mathbf{a}}_M, \check{t}_M) := \arg\min_{\mathbf{a}\in\mathcal{A},t} \quad t \quad (10)$$
$$\text{s.t.} \begin{bmatrix} \mathbf{A}(\mathbf{a})+\mathbf{\Sigma}_s^{-1} & \mathbf{e}_k \\ \mathbf{e}_k^T & t \end{bmatrix} \succeq \mathbf{0},\ k = 1,\ldots,2N_b-1.$$

Finally, the relaxed D-optimal placement can be expressed as the convex optimization problem

$$\check{\mathbf{a}}_D := \arg\min_{\mathbf{a}\in\mathcal{A}} \quad -\log\det\left(\mathbf{A}(\mathbf{a}) + \mathbf{\Sigma}_s^{-1}\right) \quad (11)$$

that can be efficiently solved via standard software.

The minimizers $\check{\mathbf{a}}_C$ of (8)-(11) do not necessarily have binary entries. A simple heuristic to obtain a binary solution is to set the largest k entries of $\check{\mathbf{a}}_C$ to 1, and zero the rest [3]. The so-acquired vector, denoted by $\hat{\mathbf{a}}_C$, belongs to the feasible set of the original non-convex problem (6), but in general it is not a minimizer of (6). It provides though the upper bound $f_C(\tilde{\mathbf{a}}_C) \leq f_C(\hat{\mathbf{a}}_C)$ for all C. Additionally, due to the relaxation, the minimizers of (8)-(11) yield also the lower bound $f_C(\check{\mathbf{a}}_C) \leq f_C(\tilde{\mathbf{a}}_C)$ for all C. When the non-negative gap $f_C(\hat{\mathbf{a}}_C) - f_C(\check{\mathbf{a}}_C)$ becomes zero, the relaxation is deemed exact in the sense that $f_C(\hat{\mathbf{a}}_C) = f_C(\tilde{\mathbf{a}}_C)$ [8].

IV. Input Data

A. Regression Matrices

Let $\tilde{\mathbf{v}} = \mathbf{v}_r + j\mathbf{v}_i$ be the $N_b \times 1$ vector of complex nodal voltages. The vector of complex nodal currents is [18]

$$\tilde{\mathbf{i}} = \mathbf{Y}\tilde{\mathbf{v}} \quad (12)$$

where $\mathbf{Y} \in \mathbb{C}^{N_b\times N_b}$ denotes the bus admittance matrix, and can be explicitly expressed in terms of the bus admittances, the line series admittances and charging susceptances, and potential tap ratios and phase shifters. Similarly, the $2N_l \times 1$ vector of complex line currents can be written as [18]

$$\tilde{\mathbf{i}}_{\text{fl}} = \mathbf{Y}_{\text{fl}}\tilde{\mathbf{v}} \quad (13)$$

where $\mathbf{Y}_{\text{fl}} \in \mathbb{C}^{2N_l\times N_b}$ is the line-to-bus admittance matrix. Note that the current flowing from bus m to bus n is not equal to the negative of the current flowing in the reverse direction. Hence, each line is considered twice in $\tilde{\mathbf{i}}_{\text{fl}}$.

The regression matrices $\mathbf{H}_n$ in (1) can now be expressed as

$$\mathbf{H}_n = \begin{bmatrix} \mathbf{e}_n^T & \mathbf{0}^T \\ \mathbf{0}^T & \mathbf{e}_n^T \\ \mathbf{S}_n\,\text{Re}(\mathbf{Y}_{\text{fl}}) & -\mathbf{S}_n\,\text{Im}(\mathbf{Y}_{\text{fl}}) \\ \mathbf{S}_n\,\text{Im}(\mathbf{Y}_{\text{fl}}) & \mathbf{S}_n\,\text{Re}(\mathbf{Y}_{\text{fl}}) \end{bmatrix} \quad (14)$$

where $\mathbf{e}_n$ is the n-th canonical vector, and $\mathbf{S}_n$ denotes the binary $L_n \times 2N_l$ matrix selecting the rows of $\mathbf{Y}_{\text{fl}}$ corresponding to the lines originating from bus n.

B. Covariance of the SCADA-based State Estimate

Conventional power meters measure subsets of nodal real and reactive power injections, real and reactive power line flows, as well as nodal voltage magnitudes. Consider M such measurements concatenated in $\mathbf{z} \in \mathbb{R}^M$ that are related to $\mathbf{v}_o$ through the function $\mathbf{h}(\cdot) : \mathbb{R}^{2N_b} \to \mathbb{R}^M$. The SCADA reading model is

$$\mathbf{z} = \mathbf{h}(\mathbf{v}_o) + \mathbf{e} \quad (15)$$

where $\mathbf{e} \sim \mathcal{N}(\mathbf{0}, \mathbf{\Sigma}_e)$ denotes the noise vector. Supposing that the SCADA-based estimate $\hat{\mathbf{v}}_s$ has converged to the MLE based on (15), the estimate $\hat{\mathbf{v}}_s$ is asymptotically (as $M \to \infty$) normal; that is, $\hat{\mathbf{v}}_s \overset{a}{\sim} \mathcal{N}(\mathbf{v}_o, \mathbf{\Sigma}_s(\mathbf{v}_o))$, where [9]

$$\mathbf{\Sigma}_s(\mathbf{v}_o) = \left(\mathbf{J}^T(\mathbf{v}_o)\mathbf{\Sigma}_e^{-1}\mathbf{J}(\mathbf{v}_o)\right)^{-1} \quad (16)$$

and $\mathbf{J}(\mathbf{v}_o) := \nabla_{\mathbf{v}}\mathbf{h}(\mathbf{v})|_{\mathbf{v}=\mathbf{v}_o}$ is the $M \times 2N_b$ Jacobian matrix of $\mathbf{h}(\mathbf{v})$ evaluated at $\mathbf{v} = \mathbf{v}_o$. Since $\mathbf{h}(\mathbf{v})$ is nonlinear, the covariance matrix in (16) depends on the actual nodal voltage values $\mathbf{v}_o$, which are unknown. To resolve this vicious cycle, one approach is to surrogate (16) by $\mathbf{\Sigma}_s(\hat{\mathbf{v}}_s)$ in (4).

For optimal PMU placement however, the goal is to solve (6) or (7) without having acquired any measurements and for all possible values of $\mathbf{v}_o$. Toward this end, the idea here is to replace $\mathbf{v}_o$ in (16) by the so-called flat voltage profile $\mathbf{v}_{\text{flat}} := [\mathbf{1}_{N_b}^T\ \mathbf{0}_{N_b}^T]^T$, commonly used for initializing state estimation algorithms [16]. For this reason, wherever $\mathbf{\Sigma}_s$ appears in the previous section it is replaced by $\mathbf{\Sigma}_s(\mathbf{v}_{\text{flat}})$. Then, the Jacobian $\mathbf{J}(\mathbf{v}_{\text{flat}})$ can be neatly expressed in terms of $\mathbf{Y}$ and $\mathbf{Y}_{\text{fl}}$. (Pertinent expressions are skipped due to space limitations.)

V. Simulated Tests

The relaxed PMU placement methods developed are evaluated numerically in this section using the IEEE 14- and 118-bus power network benchmarks [15], [18]. Regarding SCADA measurements, 50% of the bus voltage magnitudes and (real/reactive) powers are measured at buses and lines, selected uniformly at random. The covariance matrix $\mathbf{\Sigma}_e$ is modeled as diagonal: the standard deviation for voltage magnitude, bus power injections, and line power flows is 0.01, 0.015, and 0.02, respectively [18]. PMU measurements are assumed to have a diagonal $\mathbf{\Sigma}_n$ too. Compliant with SCADA readings, the standard deviation for bus voltage and line current PMU readings is 0.01 and 0.02, respectively.

For the IEEE 14-bus test case, PMU placements were evaluated for $k \in [1, 14]$ units. Figures 1-3 depict the cost values for: (i)-(ii) $f_C(\hat{\mathbf{a}}_C)$ and $f_C(\check{\mathbf{a}}_C)$ acquired by solving (7); (iii) a random placement cost; and, (iv) the cost $f_C(\tilde{\mathbf{a}}_C)$ obtained by exhaustively solving (6); all for $C \in \{A, M, D\}$. In most cases tested, $\hat{\mathbf{a}}_C$ coincided with $\tilde{\mathbf{a}}_C$, as verified by the zero gap $f(\hat{\mathbf{a}}_C) - f(\check{\mathbf{a}}_C)$. In general, $\hat{\mathbf{a}}_M$ differs from $\tilde{\mathbf{a}}_M$ by at most one unit. For the IEEE 118-bus case,

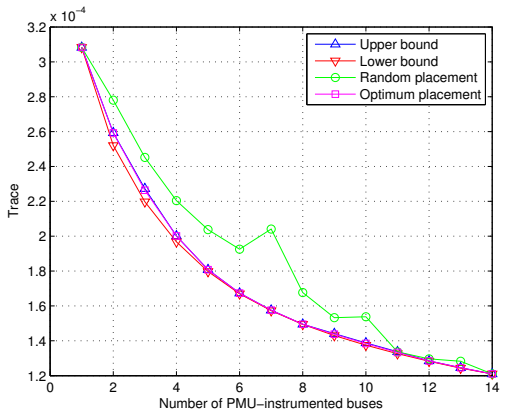

Fig. 1. IEEE 14-bus test case: A-optimal design.

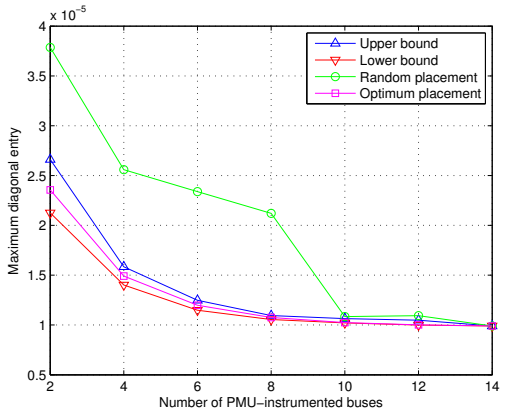

Fig. 2. IEEE 14-bus test case: M-optimal design.

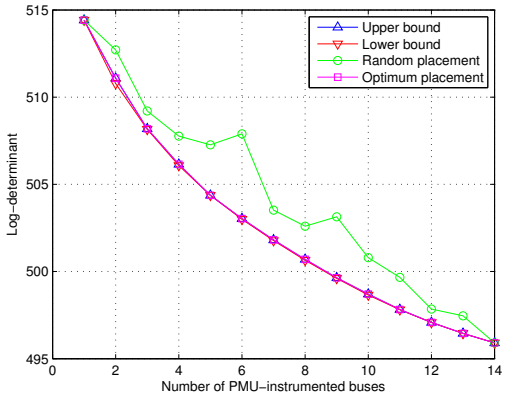

Fig. 3. IEEE 14-bus test case: D-optimal design.

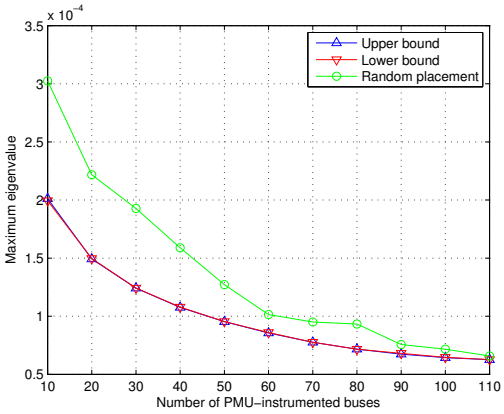

Fig. 4. IEEE 118-bus test case: E-optimal design.

the network size renders combinatorial search prohibitively complex. However, the relaxed E-optimal PMU placement is possible, as confirmed by Fig. 4.

Regarding the 14-bus test case, note first that the minimizers $\tilde{\mathbf{a}}_C$ for $C \in \{E, M\}$ do not possess a nesting property for varying k, meaning that the optimal k-placement is not necessarily a subset of the optimal $(k+1)$-one. This implies that greedy approaches cannot yield the optimum placement. Secondly, the numerical tests conducted verify the importance of the SCADA-based prior: For the A-optimal placement and $k = 14$, the trace of $\mathbf{\Sigma}_p(\tilde{\mathbf{a}}_A)$ increases from 1×10^{-4} to 2.5×10^{-4} when the prior is ignored. More critically, without the SCADA-based prior in (4), one needs $k \geq 5$ units to obtain a finite $\mathbf{\Sigma}_p(\tilde{\mathbf{a}}_A)$.

REFERENCES

[1] F. Aminifar, M. Fotuhi-Firuzabad, M. Shahidehpour, and A. Khodaei, "Probabilistic multistage PMU placement in electric power systems," *IEEE Trans. Power Delivery*, vol. 26, no. 2, pp. 841–849, Apr. 2011.

[2] T. Baldwin, L. Mili, M. B. Boisen, and R. Adapa, "Power system observability with minimal phasor measurement placement," *IEEE Trans. Power Syst.*, vol. 8, no. 2, pp. 707–715, May 1993.

[3] S. Boyd and L. Vandenberghe, *Convex Optimization*. New York, NY: Cambridge University Press, 2004.

[4] J. Y. Cai, Z. Huang, J. Hauer, and K. Martin, "Current status and experience of WAMS implementation in North America," in *Proc. IEEE Transmission and Distribution Conf.*, 2005, pp. 1–7.

[5] S. Chakrabarti, E. Kyriakides, and D. Eliades, "Placement of synchronized measurements for power system observability," *IEEE Trans. Power Delivery*, vol. 24, no. 1, pp. 12–19, Jan. 2009.

[6] J. De La Ree, V. Centeno, J. Thorp, and A. Phadke, "Synchronized phasor measurement applications in power systems," *IEEE Trans. Smart Grid*, vol. 1, no. 1, pp. 20–27, Jun. 2010.

[7] R. Emami and A. Abur, "Robust measurement design by placing synchronized phasor measurements on network branches," *IEEE Trans. Power Syst.*, vol. 25, no. 1, pp. 38–43, Feb. 2010.

[8] S. Joshi and S. Boyd, "Sensor selection via convex optimization," *IEEE Trans. Signal Processing*, vol. 57, no. 2, pp. 451–462, Feb. 2009.

[9] S. M. Kay, *Fundamentals of Statistical Signal Processing: Estimation Theory*. Upper Saddle River, NJ: Prentice Hall, 1996.

[10] Q. Li, R. Negi, and M. D. Ilic, "Phasor measurement units placement for power system state estimation: a greedy approach," in *Proc. IEEE PES General Meeting*, Detroit, MI, Jul. 2011.

[11] North American SyncroPhasor Initiative, "Synchrophasor technology roadmap," Mar. 2009.

[12] R. F. Nuqui and A. G. Phadke, "Phasor measurement unit placement techniques for complete and incomplete observability," *IEEE Trans. Power Delivery*, vol. 20, no. 4, pp. 2381–2388, Oct. 2005.

[13] A. G. Phadke and J. S. Thorp, *Synchronized Phasor Measurements and Their Applications*. New York, NY: Springer, 2008.

[14] F. Pukelsheim, *Optimal Design of Experiments*. New York, NY: Wiley & Sons, 1993.

[15] Power systems test case archive. University of Washington. [Online]. Available: http://www.ee.washington.edu/research/pstca/

[16] A. J. Wood and B. F. Wollenberg, *Power Generation, Operation, and Control*, 2nd ed. New York, NY: John Wiley & Sons, 1996.

[17] M. Zhou, V. A. Centeno, J. S. Thorp, and A. G. Phadke, "An alternative for including phasor measurements in state estimators," *IEEE Trans. Power Syst.*, vol. 21, no. 4, pp. 1930–1937, Nov. 2006.

[18] R. D. Zimmerman, C. E. Murillo-Sanchez, and R. J. Thomas, "MATPOWER: steady-state operations, planning and analysis tools for power systems research and education," *IEEE Trans. Power Syst.*, vol. 26, no. 1, pp. 12–19, Feb. 2011.